A Planar Tri-band Antenna for Ku Band Applications

Lakshmi Gayathri, Vamsi Krishna, Sri Sai Charan, Silwan and Gurpreet Kumar

School of Electronics and Electrical Engineering

Lovely Professional University

Jalandhar, India

Abstract-In this paper, a tri-band antenna for Ku-band applications is presented. This application requires a high data rate to operate for an antenna in Ku-band. The desire of having more compact made the prime choice for an antenna as a planar antenna. The features anticipate from an antenna are applications specific. The design of the proposed antenna consists of a truncated E-shaped slot, eight rectangular slots, and eight defected ground structure slots. The three frequency bands of 12.383 - 13.227 GHz, 13.643 - 14.085 GHz, 17.084 - 18.075 GHz are achieved. The simulated results of the proposed antenna are found to acceptable for gain, efficiency, and radiation pattern to ensure the suitability of the proposed antenna for Ku band applications. Furthermore, the design of the proposed antenna can be used as an element to achieve high gain in both transmission and reception modes of fixed satellite service and direct broadcast service. This paper summarizes the design, the parametric analysis and demonstrates the simulation results of the prototype antenna.

Index terms: - Satellite communications; Ku-band; Antenna; Fixed satellite service (FSS); Direct broadcast satellite (DBS); Gain; Bandwidth; Truncated E-slot

1. Introduction

In the past few years, the development of wireless communication is very rapid [1]. Due to which there is a rapid growth in satellite and radar communication systems. That resulted in high usage of a new type of antennas such as small antennas, broadband antennas, and multi-frequency antennas [2]. Generally, earth station antennas that are huge are used [1]. As they require more space these antennas were not recommended. Not only the size but also its position which is fixed at one position became the major drawback [1]. The antenna is a transducer designed to transmit or receive electromagnetic waves. Microstrip antennas have several advantages over conventional microwave antennas and therefore are widely used in many practical applications [11–13]. Now a day's communication system requires broadband antennas for a fast data transfer rate [2], Which in turn resulted in a low-profile patch antenna.It is used for multi-band performance, cheap fabrication price, and less in size [1]. A lot of patch antennas came into the picture for Ku-band satellite applications, one of those is a dual-band antenna with a single layer [1].

The two major applications of satellite communication which are given by the International Telecommunication Union (ITU) are Fixed satellite services (FSS) and Direct Broadcast Services (DBS) [1].

In the past few years, many researchers around the world have given many designs, fabrication, and optimization of antennas for FSS and DBS according to ITU norms. Some of those models are:

Dual-band antenna, the dual-band antenna consists of a U-shaped stub, L-shaped stub, and the defective ground plane. The measurement results of the antenna show that it can completely cover 3.4–3.6 GHz (200 MHz) and 5.7–6.1 GHz (400 MHz) frequency bands. This means that the antenna can meet the requirements of 5G (3.4–3.6 GHz) and 5.8G Wi-Fi (5.725–5.825 GHz). [3]

A Spiral-Fractal antenna that operates on the Ku band was proposed by Nguyen Thi. A microstrip-fed Spidron fractal patch antenna with a single-layered substrate is designed and tested. Despite the applying of one Spidron shape patch, a dual-band circularly-polarized characteristic was achieved. The results also demonstrate that the antenna exhibits an operating frequency ratio of 1.15. Therefore, the antenna can be feasibly applied for the implementation of satellite communication types that require a small frequency ratio of the upper TX band to the lower RX band. [4].

A tri-band antenna using circular disc sector for UMTS, WiMAX, and ISM band application was proposed by Mathew, A single probe-fed novel structure employing a corner truncated circular disc sector patch that generates a tri-band response using the higher-order modes is presented and experimentally studied. The multiband response can be tuned by controlling the length of the truncated edge. The antenna resonates in the UMTS, WiMAX, and the ISM 5.2 bands. The antenna is appropriate for modern wireless communication systems owing to the ease of single-layer manufacturing and the absence of any shorting posts or pins. [5].

A defected ground structure (DGS) based fractal antenna design was presented in [6]. The design is proposed for frequency ranges of 15.104–15.632 GHz, 17.336–17.912 GHz, and 18.476–19.280 GHz. ultra-wideband and tri-band antennas for satellite application at C-, X- and Ku bands are proposed the notched-band characteristics square measure exploitation to get the multiband response by making rejected bands [16–17]. It is achieved by etching two opposite U-shaped slots in the radiated patch. This property provides great freedom to select the desired frequency bands based on the total length and width of the U-slot. Nagar in [7]

From this, we can conclude that only a few designs achieved both FSS and DBS transmission and reception completely. And most of the designs are multi-layered, aperture coupled, or proximity coupled structures. It's complicated structure design, air gaps between the layers, and incompatible to use as a conformal surface antenna. By overcoming all these drawbacks, a tri-band patch antenna is proposed in this paper. The design consists of truncated E-slots and defected ground structure (DGS) slots. The designed antenna simulated results are satisfactory for the radiation pattern, impedance bandwidth, polarization, efficiency, gain, and reflection coefficient. The remaining paper is organized as follows. The details about the design and parametric study are described in Section 2 and Section 3 respectively. The simulated and results are presented in Section 4. Finally, Section 5 holds the Conclusion.

2. Design Configuration

The schematic view of the proposed antenna is shown in figure.(1) and figure.(2). The front view of the E slot and the zoomed view of the E slot are shown in figure.(1a) and figure.(1b) respectively. The back view of the antenna is shown in figure.(2). Table 1. Contains the list of all dimensions of the designed antenna. All the dimensions of the proposed antenna are taken in (mm). The substrate of the antenna is designed with a 1.6 mm thick FR-4 (lossy) substrate. CST STUDIO SUITE software tool is used for simulation of the proposed antenna.

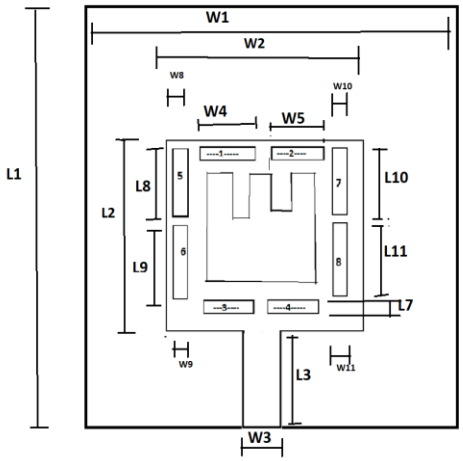

(a)

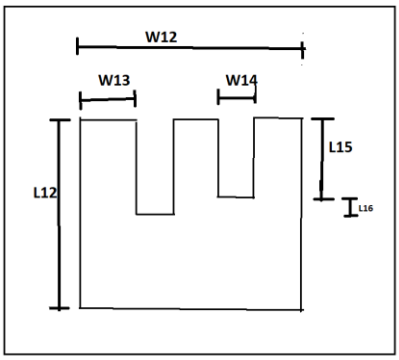

(b)

Figure.(1). Antenna design (a) Front view (b) Zoomed view of E slot

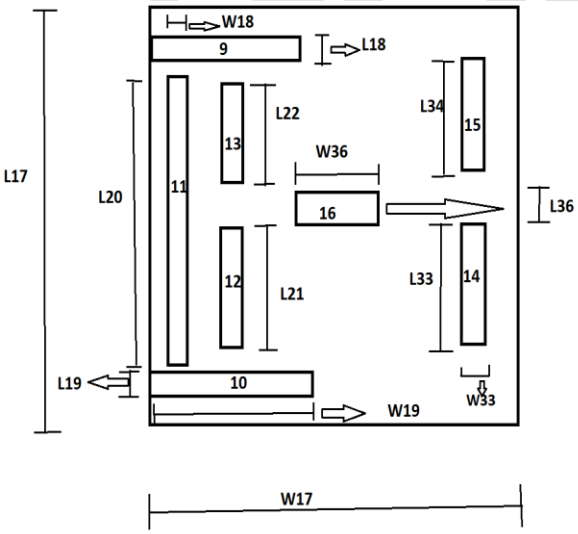

Figure.(2). Antenna design: Back view

Table 1. dimensions (in mm) of antenna

Length	Dimension	Width	Dimension
L1	20	W1	20
L2	10	W2	10
L3	5	W3	2
L4	0.5	W4	3
L5	0.5	W5	3
L6	0.5	W6	3
L7	0.5	W7	3
L8	3.5	W8	0.3
L9	3.5	W9	0.3
L10	3.5	W10	0.5
L11	3.5	W11	0.5
L12	5.1	W12	0.5
L15	2	W13	1.7
L16	2	W14	1
L17	20	W17	20
L18	0.8	W18	8.4
L19	0.8	W19	8.4
L20	12.8	W20	1
L21	5	W21	1
L22	5	W22	1
L33	6	W33	1
L34	6	W34	1
L35	5	W35	1

Initially, the design is a two C-shaped corner truncated slots as shown in figure.(3) which gives the frequency in the range of 11.40 GHz to 12.91 GHz, 13.96 GHz to15.05 GHz, and 14 GHz to 14.5 GHz for the first, second and third bands respectively. The authentic band for Direct Broad Cast Satellite (DBS) signal transmission is 17.3 GHz to17.8 GHz and hence the third band needs finer tuning. The patch design is further modified into a truncated E –shaped slot as shown in figure.(4). The shape of slots that can be provided in the patch can be U, E, S, H. but the results show that E shape (30%) more enhanced bandwidth than other shapes[14]. As a result, we achieved the frequency band 12.383 GHz to 13.227 GHz for the first band, 13.643 GHz to 14.085 GHz for the second band, 17.084 GHz to 18.075 GHz for the third band with the resonant frequency of 12.791GHz, 13.868 GHz, and 17.552 GHz respectively. Figure.(4) shows the concluding design of the Suggested antenna.

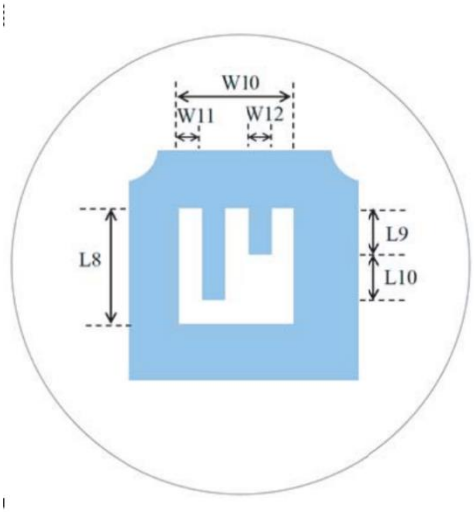

Figure.(3). Design of Two C shaped corner truncated slots on the patch

Figure.(4) shows the modified design of the patch. Figure.(4a) shows the front view of the designed patch. Figure.(4b) shows the back view of the designed patch antenna.

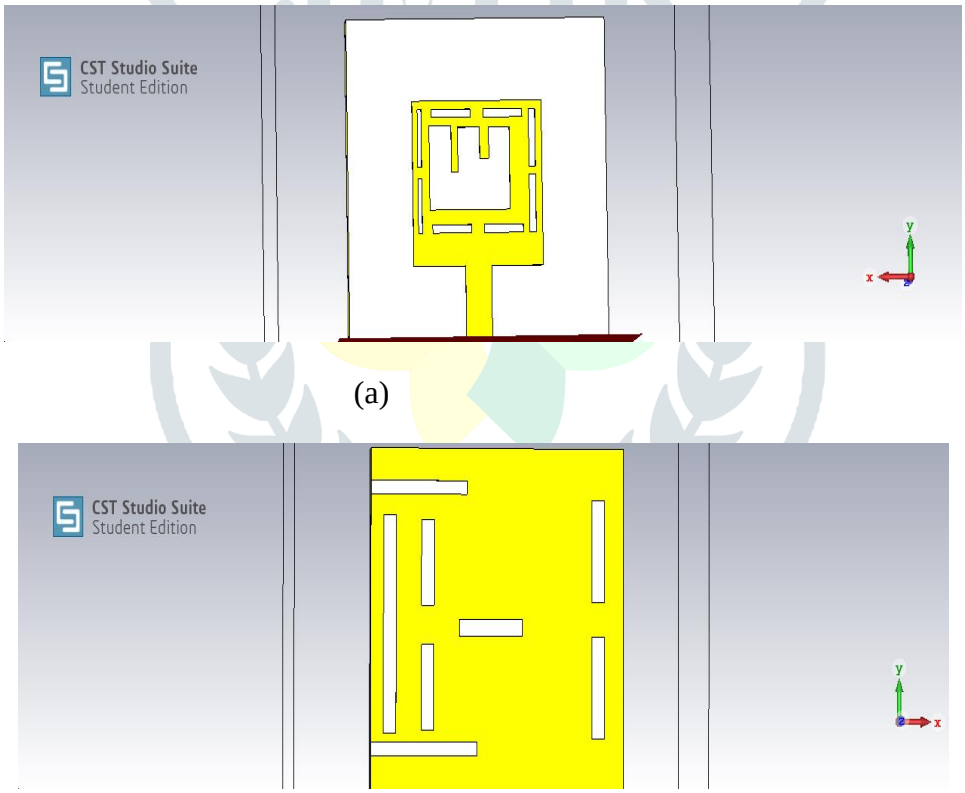

(a)

(b)

Figure.(4). Simulated antenna. (a) Front view (b) Back view

3. Parametric analysis

To enumerate the initial measurements of the design, the following general equations have been utilized. The suggested design starts with operating frequency $f1$, required permittivity Ɛr, and substrate thickness $h1$. By considering the distributed element model or the transmission line model, the Length of the patch L2 and width of the patch L2 are calculated as [7-9]

$$\Delta L = 0.412 \times h1 \frac{(\varepsilon reff + 0.3)\ 0.264 + \frac{w2}{h1}}{(\varepsilon reff - 0.258)0.8 + \frac{w2}{h1}} \quad (1)$$

The effective length of the patch is given as

$$\mathrm{L2} = \mathrm{Leff} - 2\Delta\mathrm{L} \quad (2)$$

The effective length (Leff), for resonant frequency (f1), becomes

$$\mathrm{Leff} = \frac{\mathrm{c}}{2\mathrm{f1}\sqrt{\varepsilon\mathrm{reff}}} \quad (3)$$

and

$$\varepsilon\mathrm{eff} = \frac{\varepsilon\mathrm{r}+1}{2} + \frac{\varepsilon\mathrm{r}-1}{2}\left[1 + 12\left[\frac{\mathrm{h1}}{\mathrm{W2}}\right]^{-1/2}\right] \quad (4)$$

The resonance frequency corresponds to any TM_{mn} node is given as

$$f1 = \frac{\mathrm{c}}{2\mathrm{f1}\sqrt{\varepsilon\mathrm{reff}}}\sqrt{\left(\frac{\mathrm{m}}{\mathrm{L2}}\right)^2 + \left(\frac{\mathrm{n}}{\mathrm{w2}}\right)^2} \quad (5)$$

Here, m and n are modes with respect to L1 and W1, respectively. For resonance, the width is given as:

$$W2 = \frac{c}{2f1\sqrt{\frac{\varepsilon r + 1}{2}}} \quad (6)$$

L2 ×W2 are 10×10 mm2 which is half of the center wavelength i.e., λ0/2×λ0/2 mm2 where λ0 is the center wavelength

3.1 Surface current distribution

Conceptually, the edges of the patch will have a high magnitude and the center will have the maximum current distribution at the resonant frequency. The height of the substrate is the dependent property for the distribution of the current. Figure.(5). shows the surface current distribution of the stimulating design. Figure.(5a) and Figure.(5b) show the surface current distribution for 12.791GHz. Figure.(5c) and Figure.(5d) show the surface current distribution for 13.868GHz. Figure.(5e) and Figure.(5f) show the surface current distribution for 17.552GHz. The intensity of current in the distribution is shown by the rainbow color spectrum in ampere/meter.

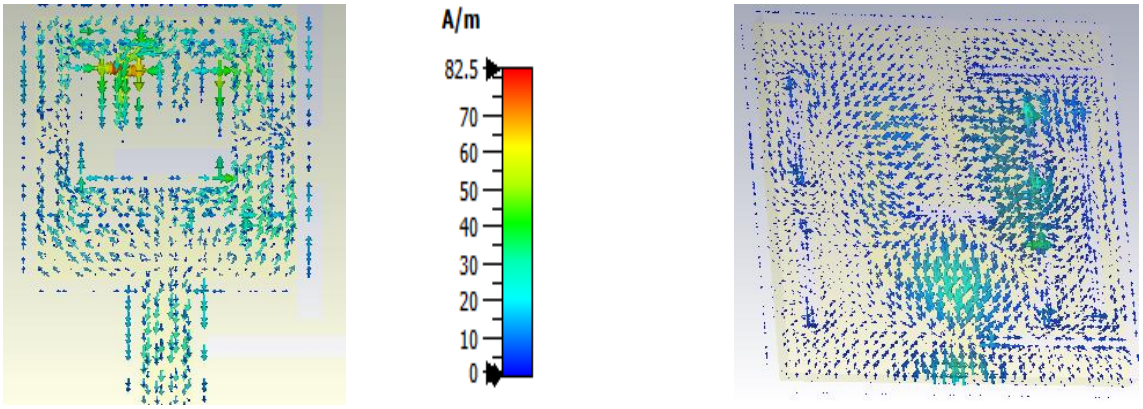

(a) (b)

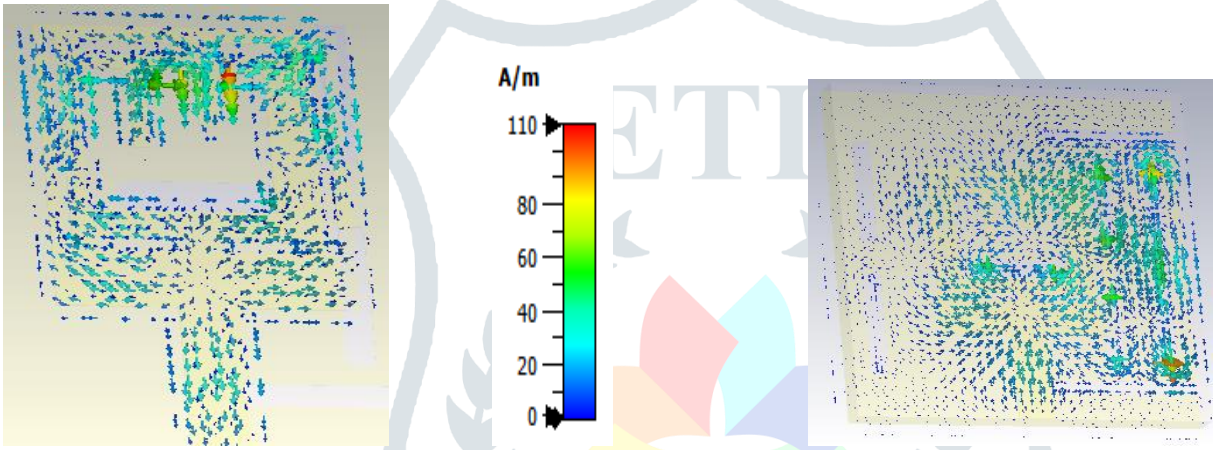

(c) (d)

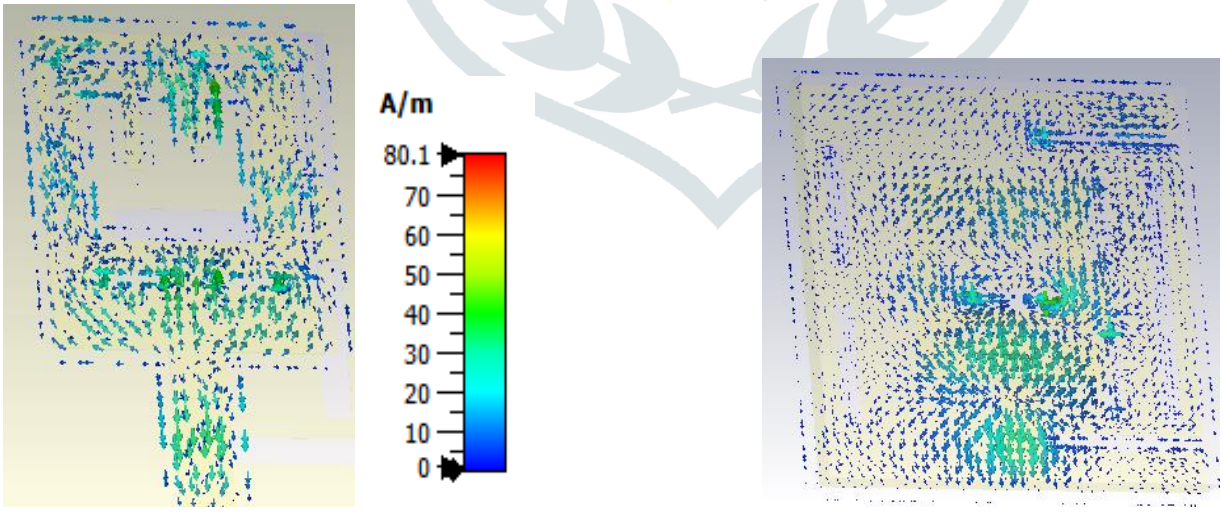

(e) (f)

Figure.(5).The current distribution across the simulated design at (a), (b) 12.791GHz , (c),(d) 13.868GHz , (e) , (f) 17.552 GHz

The magnetic field below the patch (Js=H) is equal to the electric surface current distribution at each position on the lower surface. The radiation from the patch is usually treated as radiation from two magnetic dipoles, one in the dielectric gap at each end of the patch, where the strength of the magnetic dipole field is given by the displacement current edE/dt. The magnetic dipoles run along the length of each slot and are in phase with each other. In contrast to the gaps at the ends, the sides of the patch do not radiate much. Most of the electric currents are on the underside of the patch and the ground plane directly below them, as they are on microstrip. The patch and ground currents are close together and in opposite directions, and hidden by the patch, which is why these currents don't radiate. Figure.(5a), Figure.(5c), and Figure.(5e) show the surface current distribution for the front view of the patch with a truncated E-shaped slot, slots 1–8. Figure.(5b), Figure.(5d), and Figure.(5f) show the surface current distributions for the ground plane with slots 9 to 16.

As the E shape patch antenna depends on the slot length, width, position. When these parameters are varied, it shows slot length has more effect on the resonant frequency than the slot width, position. After looking over Figure.(5a) and Figure.(5b), it has been noticed that the top portion of the E-shaped slot is having the maximum current distribution which results in the first resonant frequency 12.791GHz. By Figure.(5c) and Figure.(5d), it has been perceived that the top portion of the truncated E slot and from slot 14 to slot 15 which gives us the second resonant frequency 13.868GHz. From Figure.(5e) and Figure.5(f) it has been observed that both top and bottom portions of the E-shaped slot as well as the area of slot 16 are having the maximum current distribution leads to giving the third resonant frequency 17.552GHz.

4. Simulation results

For the initial design of Two c shaped corner truncated slots, we achieved the frequency band with central frequencies 11.7GHz and 14. 5GHz.After modification of the patch design to the truncated E slot with (1 to16) DGS slots, we achieved the frequency band with central frequencies 12.798 GHz and 13. 686 GHz. By changing the dimensions of slot 7 and slot 8 the third band of 17.552 achieved as shown in Figure.(6).

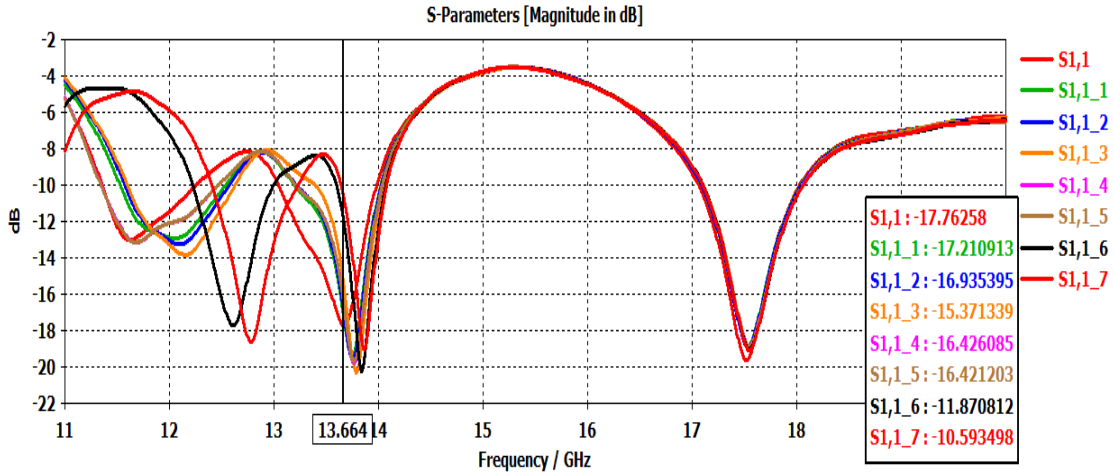

Figure.(6). Reflection Co-efficient (S11 (dB)) v/s frequency (GHz) with E-Slot, Truncated E slot, Slot 1–Slot 16 and C shaped truncated patch and ground

Figure.(7) shows the S11 v/s frequency plots for the simulated design. Observations from Figure.. 7 conclude that the proposed design works for the bands 12.383 GHz to 13..227 GHz, 13.643 GHz to 14.085 GHz, and 17.084 GHz to 18.075 GHz with resonant frequencies 12.791 GHz, 13.868 GHz, and 17.552 GHz respectively which are needed for the transmission and reception of Direct broadcast satellite (DBS) and Fixed Satellite Services (FSS).

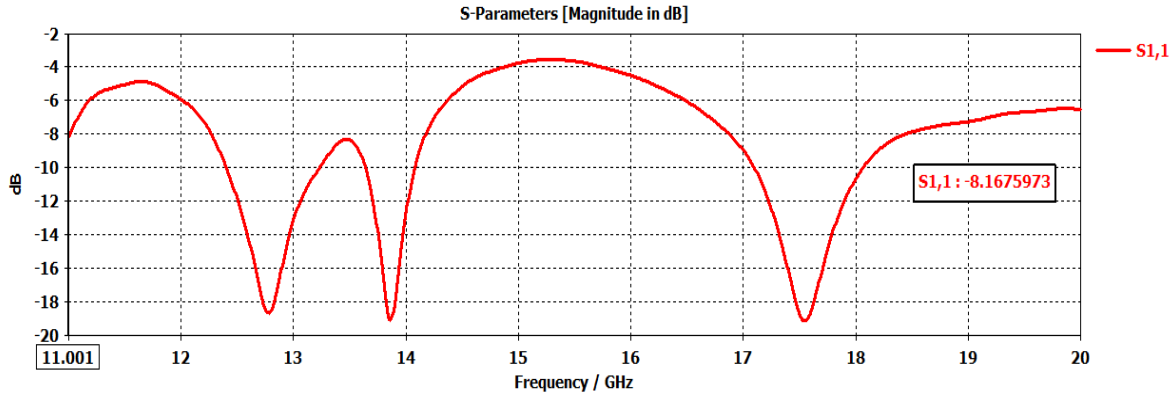

Figure.(7). S11 v/s Frequency plots

The simulated results are given in table (2). The parameters of a table (2) are lower frequency (LW), upper frequency (UW), resonant frequency (RW), and Bandwidth (BW).

Table 2. Simulated results of the first, second, and third bands for DBS and FSS.

Frequency band (GHz)	**Simulated results**			
	LW	**UW**	**RW**	**BW**
First band	12.383	13.227	12.791	0.897
Second band	13.643	14.025	13.868	0.382
Third band	17.084	18.075	17.552	0.991

4.1 Gain Vs Frequency

Gain is mostly calculated in the figure.ure of merit. Here, the gain is denoted by G or power gain Gp. we can calculate the antenna radiation pattern using gain. “Antenna gain is defined as the ratio between maximum radiation intensity of a subject antenna in a given direction to the max. the radiation intensity of an isotropic antenna” when the same amount of power is applied to both antennas. The gain value indicates how much your antenna succeeded while converting the input power into radio waves in a specific direction and how it converts the radio waves into electrical form at the receiver side. Sometimes, the gain is discussed as a function of angle. By the gain value, we can know how much amount of signal boosting is provided to the input by the antenna.

It helps at the receiver stage, how much power is required to reproduce the same transmitted signal from the channel. Figure.(8) demonstrates the Gain and frequency plot of the simulated design.

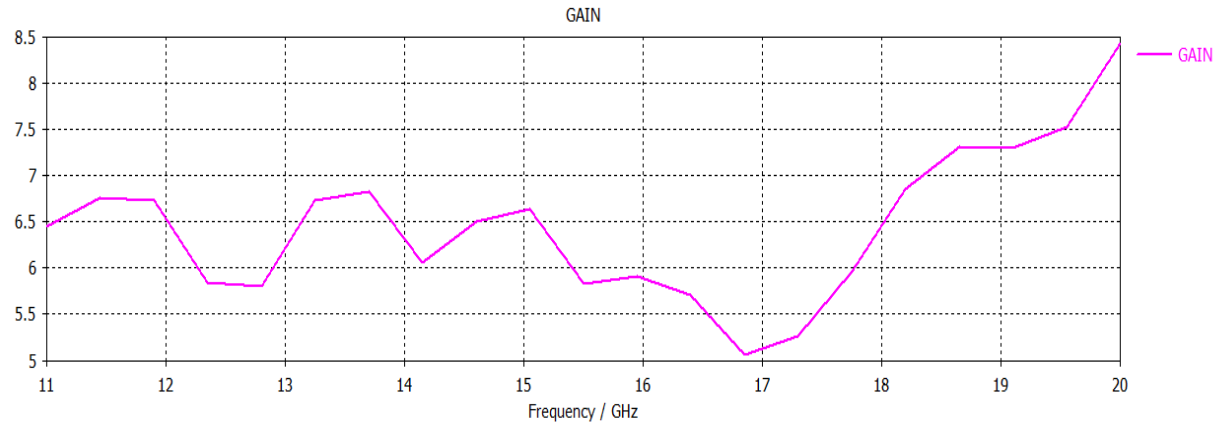

Figure.(8). Gain (dbi) vs frequency (GHz) plot

5. Conclusion

In this manuscript, a small-size tri-band antenna has been designed and simulated for Ku band applications. In this design eight rectangular slots in the patch, a truncated E-shaped slot and eight defected ground structure (DGS) slots have been used By utilizing the proposed design, we achieved the frequency bands which are obligatory for the transmission of Direct Broadcast Satellite (DBS) and Fixed satellite service (FSS) signals. The antenna design suggested in this manuscript can be utilized as an element in an array configure.uration to achieve the enhanced gain required for transmission and reception of Fixed satellite services (FSS) and Direct broadcast satellite (DBS).

IV. REFERENCES

1. T. A. Milligan, Modern Antenna Design, New York: McGraw-Hill, 1985

2. Wutthipong Thanamalapong, Chuwong Phongcharoenpanich and Suthasinee Lamultree" A Tri-Band Antenna for 2.4/5 GHz WLAN and Ku-Band Applications" IEEE

3. Mao, Y., S. Guo, and M. Chen, "Compact dual-band monopole antenna with the defected ground plane for Internet of things," IET Microwaves, Antennas & Propagation, Vol. 12, No. 8, 1332–1338, 2018.

4. Nguyen Thi, T., K. C. Hwang, and H. B. Kim, "Dual-band circularly-polarised Spidron fractal microstrip patch antenna for Ku-band satellite communication applications," Electronics Letters, Vol. 49, No. 7, 444–445, 2013.

5. Mathew, S., R. Anitha, U. Deepak, C. K. Aanandan, P. Mohanan, and K. Vasudevan, "A compact tri-band dual-polarized corner-truncated sectoral patch antenna," IEEE Transactions on Antennas and Propagation, Vol. 63, No. 12, 5842–5845, 2015.

6. Gupta, A., H. D. Joshi, and R. Khanna, "An X-shaped fractal antenna with DGS for multiband applications," International Journal of Microwave and Wireless Technologies, Vol. 9, No. 5, 1075– 1083, 2017.

7.Naghar, A., O. Aghzout, M. Essaaidi, A. Alejos, M. Sanchez, and F. Falcone, "Ultra-wideband and tri-band antennas for satellite applications at C-, X-, and Ku bands," Proceedings of 2014 Mediterranean Microwave Symposium (MMS2014), 1–5, IEEE, December 2014.

8.Jang, H. K., J. H. Shin, and C. G. Kim, "Low RCS patch array antenna with electromagnetic

bandgap using a conducting polymer," IEEE International Conference in Electromagnetics AdvanceApplications, 140143, Sydney, Australia, 2010.

9.Dhawan Singh and Viranjay M. Srivastava, "Comparative analyses for RCS of patch antenna using shorted stubs metamaterial absorber," Journal of Engineering Science and Technology (JESTEC), Vol. 13, No. 11, 3532–3546, November 2018.

10 . Balanis, C. A . , Antenna Theory; Analysis and Design, 3rd Edition, John Wiley and Sons Inc, New York, 2005.

11 . James j . , and P.S. Hall (Eds), Handbook of microstrip antenna, Peter Peregrinus, London, UK, 1989.

12 . Ramesh Garg, Prakash Bartia, Inder Bahl, Apisak Ittipiboon, ''Microstrip Antenna Design Handbook'', 2001, pp 1-68, 253 - 316.

13 . Robert A . Sainati, CAD of Microstrip Antennas for Wireless Applications, Artech House Inc, Norwood, MA, 1996.

14 . Atser A. Roy, Joseph M. Môm, Gabriel A . Igwue, " Enhancing the Bandwidth of a Microstrip Patch Antenna using Slots Shaped Patch", American Journal of Engineering Research (AJER), Vol.2, Issue 9, pp23 - 30, July 2013.

15 . Josko Kucan, Miroslav Joler, "Impact of slot dimensions on the resonant frequencies of rectangular microstrip antennas", IEEE transaction, vol. 45 Issue. 5, pp. 456 - 467, July 2013.

16 . Khare, A. and R. Nema, " Triple band parasitic array antenna for C – X – Ku - band application using out - of - phase coupling approach, " International Journal of Antennas and Propagation, 2014.

17 . Dhakad, S . K. and T. Bhandari, "A hexagonal broadband compact microstrip monopole antenna for C band, X band and Ku band applications, " 2017 International Conference on Computing, Communication and Automation (ICCCA), 1532 - 1536, IEEE, May 2017